

# Triplet Pairing in pure neutron matter

Sarath Srinivas\* and S. Ramanan†

*Indian Institute of Technology Madras, Chennai, India.*

(Dated: August 2, 2021)

We study the zero temperature BCS gaps for the triplet channel in pure neutron matter using Similarity Renormalization Group (SRG) evolved interactions. We use the dependence of the results on the SRG resolution scale, as a tool to analyze medium and many-body corrections. In particular, we study the effects of including the three-body interactions at leading order, which appear at N<sup>2</sup>LO in the chiral EFT, as well as that of the first-order self-energy corrections on the zero temperature gap. In addition we also extract the transition temperature as a function of densities and verify the BCS scaling of the zero temperature gaps to the transition temperature. We observe that the self-energy effects are very crucial in order to reduce the SRG resolution scale dependence of the results, while the three-body effects at the leading order do not change the two-body resolution scale dependence. On the other hand, the results depend strongly on the three-body cut-off, emphasizing the importance of the missing higher-order three-body effects. We also observe that self-energy effects reduce the overall gap as well as shift the gap closure to lower densities.

## I. INTRODUCTION

Neutron stars are dense stellar objects that are formed after gravitational collapse of a massive star. The star is mainly composed of asymmetric matter, which is neutron rich with a small percentage of protons whose positive charge is compensated by an equal number of electrons. The density of matter in the star increases radially inwards reaching values greater than the nuclear saturation density at the center. The models explaining the cooling rate of neutron stars suggest the existence of superfluid phases of neutrons in the inner crust and outer core where they form Cooper pairs [1–9]. Pairing occurs between neutrons in the  $^1S_0$  channel which is attractive for  $k_F < 1.7 \text{ fm}^{-1}$ , where  $k_F$  is the Fermi momentum. At higher densities, pairing between neutrons occurs in the triplet channel  $^3P_2 - ^3F_2$ . The density dependence of neutron pairing in the different partial wave channels is not well understood and is a problem of interest in low energy nuclear physics. Pairing between protons is still an open problem, as one has to deal with the low densities of protons interacting in a medium of high density neutrons.

Understanding pairing in the triplet channel is very important to explain the cooling of neutron stars. For example, the recent sudden cooling of Cassiopeia-A can be explained by the existence of the superfluid neutrons in the triplet channel [9–11]. By analyzing the archival data of the Chandra X-ray observatory, it was documented that the surface temperature of Cassiopeia-A had suddenly decreased by a factor of  $\sim 3.6\%$ . Although observational uncertainties can change this rate to  $\sim 2.9\%$  [12], one still requires the neutrons in the triplet channel to be in the superfluid phase with a moderately high transition temperature, to make theoretical predictions match

observations. These predicted rates of decline in the surface temperature control the width of the density profile of the transition temperature,  $T_c$ , as well the peak value of  $T_c$  as a function of density. A large value of  $T_c$  allows for the star to enter the superfluid phase early in its thermal evolution, while a moderate value allows for a rapid cooling in the intermediate years. These observations motivate the recent renewed interest in the superfluid triplet channel of pure neutron matter [17, 18, 20, 21].

The triplet channel is particularly challenging: the reason being that the gaps (within the BCS approximation), remain open at much higher densities, usually in the range,  $1 \text{ fm}^{-1} < k_F < 3.5 \text{ fm}^{-1}$ . We define the BCS approximation as one where the two-body free space interaction is used as input to the BCS gap equation, while a free-spectrum is used for the intermediate single particle states. In the two-body sector, a typical phenomenological nucleon-nucleon interaction is constrained by the two-body scattering data up to 350 MeV lab energies or equivalently up to  $2.0 \text{ fm}^{-1}$  in momentum scale. In addition to the phenomenological interactions, there are EFT based chiral interactions where the low-energy constants are fit to the two-body data and these interactions have a built-in EFT cut-off that specifies the range of momenta for which the interactions are valid. The biggest challenge when using these standard two-body interactions to study pairing in the triplet channel is that for the range of momenta corresponding to the densities where the triplet gaps exist, these high-precision two-body interactions no longer yield equivalent phase shifts in free space (Fig.1 in [14] and Fig. 4 in this work). This results in model dependent gaps in the triplet channel [14, 15, 17, 18, 20, 21]. The uncertainties in the predicted gap values are influenced by the fact that the input interactions are no longer phase-shift equivalent in free space, in addition to the missing many-body/medium corrections.

While pairing in the  $^1S_0$  channel has been extensively studied, for example [13, 15, 16], pairing in higher partial waves, especially the triplet channel is not very well understood. Recently, there has been renewed interests

---

\*Electronic address: saraths@physics.iitm.ac.in

†Electronic address: suna@physics.iitm.ac.in

in this channel [14, 17–21]. In [17], the authors study the triplet pairing in pure neutron matter within the BCS framework, taking into account the effect of short-range correlation via the  $Z$ -factor, while [20, 21] takes into consideration both the short-range and long-range correlations using self-consistent Green’s function techniques and Fermi Liquid theory respectively. In both these approaches there is a remarkable decrease in the overall magnitude of the angle-averaged triplet gaps as well as the gap closure shifts to lower densities. Recently, Maurizio et al. [18, 19] have studied the gap equation in the singlet and in the triplet channel for both symmetric nuclear matter and pure neutron matter using chiral interactions at N3LO and its renormalization group evolved low-momentum interactions (SRG) for the symmetric matter (singlet and triplet), while for the triplet channel in pure neutron matter, they have documented the gaps for different two-body interactions, including the chiral interactions and have explored the effects of adding chiral three-body interactions at N2LO as well as that of including an effective mass. They solve the BCS gap equation following the numerically stable procedure of Khodel et al. [30].

It is customary to work in a partial wave basis and in this basis the gap depends on  $(j, l, m)$ , where  $j$  is the total angular momentum,  $l$  is the orbital angular momentum and  $m$  is the projection of  $j$ . In the triplet channel the study of gaps with  $m$  dependence and partial wave mixing are by themselves very interesting in the context of cooling and transport. While the transition temperature is unaffected by the spin of the paired state, the form of the gap below  $T_c$  very much depends on whether the pairing occurs in the spin singlet or in the spin triplet channels. Such problems have been studied in the past in [25–27] and recently in [28], where the possibility of gaps with a node that lead to special collective modes have been discussed.

In this study, we re-visit the problem of pairing in pure neutron matter, a close approximation to the highly asymmetric neutron stars, as a function of density. Our work lays special emphasis on the pairing in the triplet channel  ${}^3P_2 - {}^3F_2$ , thereby extending the work of Maurizio et al. [18]. We use the angle-averaged approximation to the triplet gap, along with the assumption that the different partial waves contribute in non-overlapping intervals, as a starting point. Although working in this approximation is a standard first step, and is a useful one numerically, we wish to emphasize that the effects of the  $m$  dependence as well as allowing the different  $j$  to mix could have very interesting effects [26, 30]. But this is beyond the scope of the current work.

We use SRG-evolved interactions as input to the triplet channel gap equation. SRG evolution [38, 39] (and references within) has the advantage of decoupling low and high momenta via unitary transformations of the Hamiltonian, while preserving observables, which are the two-body phase shifts and the deuteron binding energy in the two-body sector as a function of a flow parameter  $s$ ,

where  $s^{-1/4}$  has the dimensions of momentum. In the canonical implementation of SRG, the evolution drives the interaction matrix elements towards the diagonal, leaving a low-momentum block and a high momentum tail [40]. Usually one uses a parameter  $\lambda = s^{-1/4}$ , which is a measure of the spread of the off-diagonal strength and sets the SRG resolution scale. This identification allows one to connect to the older class of renormalization group based low-momentum interaction,  $V_{\text{low } k}$ , specified by the momentum cut-off  $\Lambda$ . For more details on the SRG evolution, we refer the reader to the appendix .

Therefore, when we compare the gaps for different SRG resolution scale,  $\lambda$ , we have by construction removed the contribution of the two-body phase shift inequivalence to the  $\lambda$  dependence. This allows one to use the dependence of the gap on  $\lambda$  as a tool to estimate the scale of the missing physics such as many-body and/or medium dependencies. We note that the gaps obtained for different densities and SRG resolution scales will depend on the bare interactions, but we wish to only study global trends across different bare interactions. In particular, we compare in this study the SRG resolution scale dependence trends for the N3LO EM 500 [41] class of SRG interactions and the AV<sub>18</sub> [42] class of SRG interactions so as to have examples from an EFT inspired interaction as well as a phenomenological one. We add that the N3LO EM 500 interaction has a chiral cut-off of 500 MeV  $\sim 2.5 \text{ fm}^{-1}$ . As a result, one needs to be careful while interpreting the results for the chiral interaction as  $k_F$  approaches values close to the cut-off. In this work, we make a more conservative estimate for the build-up of the errors and interpret results using the N3LO interactions beyond  $k_F \sim 2.0 \text{ fm}^{-1}$  with caution.

We augment the N3LO EM 500 bare as well as its SRG evolved counterparts by the leading order chiral three-body force, that occurs at N2LO in the chiral expansion. The leading order unevolved three-body force is regulated by an exponential regulator, parameterized by a three-body cut-off,  $\Lambda_{3\text{NF}}$ . The three-body interaction is added to the two-body chiral interaction as a density dependent two-body force, obtained by integrating the third particle over the filled Fermi sea [16]. By using a leading order unevolved three-body force, we have left out higher-order three-body effects as well as that of the induced three-body. Our motivation for the three-body study undertaken in this work is to primarily test the approximation of adding unevolved leading order three-body forces as a density dependent two-body force for the range of densities relevant to the triplet gaps in pure neutron matter. In addition, the current prescription for adding the leading order three-body force, gives an additional three-body cut-off. Therefore one can use the dependence on the three-body cut-off as a tool to estimate the higher-order three-body corrections, in addition to studying the effect of the three-body force to the triplet pairing gaps. There have been several studies in the past for the triplet channel of pure neutron matter where the two-body forces have been augmented by a density de-

pendent phenomenological three-body force [22, 23]. It has been observed in these studies that the addition of the three-body force enhances the triplet pairing gap, which is what we see in our work as well. However, we would like to emphasize that our study here with the leading order chiral three-body force is only exploratory and by no means complete.

We solve the angle-averaged gap equation using the numerically stable procedure outlined by Khodel et al. [18, 30]. Alternatively, one can extract the angle-averaged gap by picking out the poles of the in-medium  $T$  matrix through the Weinberg eigenvalue method [31] developed in [36] for the singlet channel. As a proof of principle, we generalize the eigenvalue method for the triplet channel and show that the gaps obtained are identical to the angle-averaged ones got by solving the gap equation in the triplet channel. The Weinberg eigenvalue method can be extended to finite temperatures as in [37], where it was applied to obtain the transition temperature for the  $^1S_0$  channel. In this work, we extract the transition temperature as a function of  $k_F$  for the triplet channel.

This paper has been organized as follows. In section II we discuss how the gap equation in the partial wave basis can be solved in a numerically stable way, recapitulating the approach presented in [18, 30] and we present the method of the Weinberg eigenvalues in order to extract the zero temperature angle-averaged gaps. In section II C we generalize the eigenvalue method to finite temperatures. We motivate the advantage of using SRG-evolved low-momentum interactions and present the main results of the paper and detail the higher-order corrections that we wish to include in section III. We summarize our results and list out our long-term goals in section IV. Throughout this paper we work in units where  $c = 1$  and  $\hbar^2/m_N = 1$ .

## II. THE BCS PAIRING GAP

It is well known that an attractive interaction between fermions favors the formation of Cooper pairs, which then condense leading to an instability of the normal ground state. Since the  $NN$  interaction has attractive and repulsive pieces, one expects pairing in different partial wave channels as a function of density. The BCS gaps at zero temperature can be extracted by numerically solving the BCS gap equation in the respective partial wave channels [18, 30].

One can alternatively pick out the poles of the  $T$  matrix equation for energies around the Fermi surface [36]. This is done by looking at the eigenvalue equation for  $VG_0(E)$ , where  $G_0(E)$  is the two-particle non-interacting Green's function. The poles of the  $T$  matrix are signaled by the eigenvalues of  $VG_0(E)$  approaching 1. Therefore if one interprets the formation of Cooper pairs as the formation of bound states at the Fermi surface with complex energies, then the imaginary part yields the gap [36].

In the following subsections we present both the ap-

proaches for completeness.

### A. The Gap equation and its numerical solution

The BCS gap equation that allows the estimation of the energy gap is given by:

$$\Delta(\mathbf{k}) = - \sum_{\mathbf{k}'} \langle \mathbf{k} | V | \mathbf{k}' \rangle \frac{\Delta(\mathbf{k}')}{2E(\mathbf{k}')}, \quad (1)$$

where  $E(\mathbf{k})^2 = \xi(\mathbf{k})^2 + \Delta(\mathbf{k})^2$  and  $\xi(\mathbf{k})$  is the single particle energy measured from  $E_F$ , the Fermi energy, i.e.,  $\xi(\mathbf{k}) = e(\mathbf{k}) - E_F$ . For simplicity, we assume a free spectrum for the single particle energies to begin with and will consider corrections to this assumption in the later sections of this work. We are interested in the value of the gap at the Fermi surface as a function of  $k_F$ .

Working in a partial wave basis, the gaps in the triplet channel, depend on  $j$ ,  $l$  and  $m$  [30]. Upon angle averaging, we have the following equation:

$$\Delta_l(k) = \sum_{l'} \frac{(-1)^N}{\pi} \int_0^\infty q^2 dq V_{ll'}(k, q) \frac{\Delta_{l'}(q)}{E(q)}, \quad (2)$$

where  $N = 1 + \frac{(l-l')}{2}$  and  $E(k)^2 = \xi(k)^2 + D(k)^2$  and  $\xi(k) = e(k) - E_F$ . In addition, following [18], we have also assumed in Eq. (2), that the gaps with different  $l$  and  $j$  do not overlap and hence we have  $D(k)^2 = \sum_l \Delta_l(k)^2 = \Delta_1(k)^2 + \Delta_3(k)^2$  for the  $^3P_2 - ^3F_2$  channel. Setting  $l = l'$  in Eq. (2), we retrieve the gap equation for the uncoupled channels in the partial wave basis. We note that the intermediate states have momenta in the range  $[0, \infty)$ . However, in practice, the two-body interactions have non-zero matrix elements up to some maximum momentum,  $k_{\max}$ , which in turn sets the range of  $q$ . For notational simplicity, the limits on the intermediate state momenta will be henceforth suppressed in our discussion. In order to solve the gap equation in a numerically stable way, we resort to a quasi-linear method as in [30] which was used recently by Maurizio et al. [18, 30]. We begin by defining an auxiliary potential  $W_{ll'}(k, k')$  such that

$$W_{ll'}(k, k') = V_{ll'}(k, k') - v_{ll'} \phi_{ll'}(k) \phi_{ll'}(k'), \quad (3)$$

where  $\phi_{ll'}(k) = \frac{V_{ll'}(k, k_F)}{V_{ll'}(k_F, k_F)}$  and  $v_{ll'} = V_{ll'}(k_F, k_F)$  and by construction the auxiliary potential in Eq. (3) vanishes if  $k$  or  $k'$  lies on the Fermi surface. The gap equation becomes:

$$\begin{aligned} \Delta_l(k) - \sum_{l'} \frac{(-1)^N}{\pi} \int q^2 dq W_{ll'}(k, q) \frac{\Delta_{l'}(q)}{E(q)} \\ = \sum_{l'} D_{ll'} \phi_{ll'}(k), \end{aligned} \quad (4)$$

and the coefficients satisfy,

$$D_{ll'} = \frac{(-1)^N}{\pi} v_{ll'} \int q^2 dq \phi_{ll'}(q) \frac{\Delta_{l'}(q)}{E(q)}. \quad (5)$$

The gap is defined as,

$$\Delta_l(k) = \sum_{l_1 l_2} D_{l_1 l_2} \chi_l^{l_1 l_2}(k), \quad (6)$$

and

$$\begin{aligned} \chi_l^{l_1 l_2}(k) &= \sum_{l'} \frac{(-1)^N}{\pi} \int q^2 dq W_{ll'}(k, q) \frac{\chi_{l'}^{l_1 l_2}(q)}{E(q)} \\ &= \delta_{ll_1} \phi_{l_1 l_2}(k), \end{aligned} \quad (7)$$

where  $\delta_{ll_1}$  is the Kronecker delta. By construction,  $\chi_l^{l_1 l_2}(k_F) = \delta_{l, l_1}$  for any value of  $l_2$ , since the potential  $W_{ll'}(k_F, q) = 0$  and  $\phi_{l_1 l_2}(k_F) = 1$ . We write the energy denominator of Eq. (7) as  $E(q) = \sqrt{\xi^2(q) + \delta^2}$  where  $\delta$  is a scale factor and the final result is independent of the choice of  $\delta$  [18]. Eqs. (5), (6) and (7) are solved self-consistently to yield the gaps (or the angle-averaged gaps for the triplet channel). The numerical advantage that is gained by the method of separation by Khodel et al. is that the singular part of the gap equation, where the singularity arises for small values of the gap as one approaches the Fermi surface, is separated from the gap equation via the function  $\chi_k^{l_1 l_2}(k)$ . Further, as in (Eq. (7)), these functions involve integrals over the auxiliary potential, which by construction go to zero on the Fermi surface. As a result, the functions  $\chi_l^{l_1 l_2}(k)$  are insensitive to the quantity  $\delta$  used as a first guess while solving Eqs. (5), (6) and (7) self-consistently.

## B. Stability Analysis

As an alternative to solving the gap equation, one can also look for the poles of the in-medium  $T$  matrix. The idea is to view pairing as a non-perturbative phenomena that leads to the instability of the normal ground state, resulting in the divergence of the particle-particle ladder series. The poles of the  $T$  matrix are located by studying the eigenvalue equation for  $G_0(E)V$ , which is the operator that is iterated in the Born series expansion of the  $T$  matrix, that is:

$$\begin{aligned} T(E) &= V + VG_0(E)T(E) \\ &= V + VG_0(E)V + VG_0(E)VG_0(E)V \\ &\quad + \dots, \end{aligned} \quad (8)$$

where  $G_0(E)$  is usually the two-particle non-interacting free space Green's function. Therefore, if one picks a basis where  $G_0(E)V$  is diagonal, i.e.

$$G_0(E)V|\Gamma\rangle = \eta(E)|\Gamma\rangle, \quad (9)$$

then the Born series expansion for the  $T$  matrix becomes:

$$T(E) = V(1 + \eta(E) + \eta(E)^2 + \dots), \quad (10)$$

which converges if  $|\eta(E)| < 1$ . We can immediately see that if  $E$  is a true bound state of the potential, the eigenvalue equation, Eq. (9), becomes the Schrödinger's equation for the bound state and therefore for that energy  $E$ , the corresponding eigenvalue equals 1.

The eigenvalues of the operator  $G_0(E)V$ , referred to as the Weinberg eigenvalues in the literature, allow one to track the sources of non-perturbative physics in the interaction  $V$ , which show up as eigenvalues larger than 1, hence rendering the Born series divergent [32]. One can also use the eigenvalues as in [34–36] to determine the momentum independent pairing gap.

Pairing leads to an instability in the normal ground state resulting in the divergence of ladder diagrams, which should be reflected in the divergence of the Weinberg eigenvalues as  $E \rightarrow 2E_F$ . Close to the Fermi surface, one needs to consider hole-hole scattering in addition to particle-particle scattering. Therefore, in order to extract the pairing gap using the Weinberg eigenvalues, one replaces the two-particle free space Green's function by the in-medium non-interacting particle-particle hole-hole Green's function at zero center of mass momentum. When one studies the eigenvalues of the operator  $G_0(E)V$ , it is seen that as a function of  $E$ , the eigenvalues diverge as  $E \rightarrow 2E_F$  [34–36]. With the view that the pairing instability is due to the formation of bound states of Cooper pairs which then condense, we note that the two-body non-interacting particle-particle hole-hole Green's function can only accommodate the new bound state (Cooper pair) on the imaginary axis as the real axis has the particle-particle continuum for  $E > 2E_F$  and the hole-hole continuum for  $E < 2E_F$  [35]. As a result, if one replaces the  $E$  in the energy denominator of the Green's function by  $2E_F + iE_0$  and adjusts  $E_0$ , then value of  $E_0$  for which  $|\eta(2E_F + iE_0)| = 1$  gives the pairing gap [36].

For the uncoupled channels, one solves the following eigenvalue equation in the partial-wave basis:

$$\begin{aligned} \frac{2}{\pi} \int q^2 dq V_{ll}(k, q) \left[ \frac{\theta(q - k_F)}{E - q^2 + i\epsilon} \right. \\ \left. - \frac{\theta(k_F - q)}{E - q^2 - i\epsilon} \right] \Gamma_l(q, E) = \eta_l(E) \Gamma_l(k, E) \end{aligned} \quad (11)$$

where  $E = 2E_F + iE_0$ . We then dial in complex energies and pick out the value  $E_0$  such that  $|\eta_l(2E_F + iE_0)| = 1$ .

This procedure is called the stability analysis and was employed to extract the  $^1S_0$  pairing gap at zero temperatures [36].

In order to extract the gaps for the coupled channels, Eq. (11) is generalized as follows:

$$\begin{aligned} \frac{2}{\pi} \sum_{l'} \int q^2 dq V_{ll'}(k, q) \left[ \frac{\theta(q - k_F)}{E - q^2 + i\epsilon} \right. \\ \left. - \frac{\theta(k_F - q)}{E - q^2 - i\epsilon} \right] \Gamma_{l'}(q, E) = \eta_l(E) \Gamma_l(k, E). \end{aligned} \quad (12)$$

Once again  $E = 2E_F + iE_0$  and one dials  $E_0$  searching for an eigenvalue such that  $|\eta_l(2E_F + iE_0)| = 1$  analogous to the uncoupled case.

We will see in sect III that the zero temperature gaps extracted for the  $^1S_0$  and the  $^3P_2 - ^3F_2$  channels are equivalent to the corresponding gaps obtained from the

gap equation. Therefore the stability analysis provides an alternate method to extract the pairing gaps.

We also note that the stability method can be extended to include beyond BCS corrections as well as to finite temperatures (see section. II C). In principle, the numerical cost for the eigenvalue search is comparable to solving the BCS gap equation. Both are very sensitive to the distribution of the momentum grid points, especially around  $k_F$ . Although the numerical costs are the same for the two methods, we find that solving the BCS gap equation through the method of Khodel et al. is very robust numerically for small values of the gap by construction. In the stability method, the smallest possible gap is limited by the denominator becoming singular around  $k_F$ . Hence one might observe that the gaps open and close abruptly compared to the gaps obtained by solving the BCS equation through the method of Khodel et al. In addition, we also note that the Khodel method is applicable for any interaction [30], while the eigenvalue method works very well for interactions that are soft such as, SRG evolved interactions at lower SRG resolution scales, chiral interactions etc [36]. For such soft interactions, the large eigenvalue close to  $E_F$  is associated with pairing, but for interactions where repulsive pieces exist, such as bare  $AV_{18}$  in the  $^1S_0$  or in the  $^3P_2 - ^3F_2$  channels the stability method is more involved, as the large values for  $|\eta(E)|$  could arise due to both the pairing instability as well as due to the presence of short-range pieces that renders an “in-medium” Born series divergent. In this case, one needs to impose additional constraints on the phase of the eigenvalue.

In the following section, we discuss the extension of the Weinberg eigenvalue method to finite temperatures.

### C. Transition temperature via Weinberg Eigenvalues

The method of obtaining the pairing gaps at zero temperatures via the Weinberg eigenvalues can be easily extended to finite temperatures as in [37]. This is done by replacing the zero temperature Green’s function by the finite temperature counterpart evaluated at zero center of mass momentum:

$$G_0(\mathbf{k}, \omega) = \frac{1 - 2f(\xi(\mathbf{k}))}{\omega - 2\xi(\mathbf{k}) + i\eta}. \quad (13)$$

where  $f(\xi) = 1/(e^{\beta\xi} + 1)$  is the Fermi-Dirac distribution function and  $\omega = E - 2\mu$ ,  $\xi(\mathbf{k}) = e(\mathbf{k}) - \mu$  are the energies measured from the chemical potential. While working in a partial wave basis with the free-particle spectrum for the single particles, one obtains the following Weinberg eigenvalue equations at finite temperature applicable to the uncoupled and coupled channels respectively:

$$\frac{2}{\pi} \int q^2 dq V_{ll}(k, q) G_0(q, \omega) \Gamma_l(q, \omega) = \eta_l(\omega) \Gamma_l(k, \omega), \quad (14)$$

and

$$\frac{2}{\pi} \sum_{l'} \int q^2 dq V_{ll'}(k, q) G_0(q, \omega) \Gamma_{l'}(q, \omega) = \eta_l(\omega) \Gamma_l(k, \omega), \quad (15)$$

where we have suppressed the dependence on  $\mu$  and  $T$  in Eqs. (14) and (15) for notational simplicity. At finite temperatures, the largest eigenvalue that equals 1 is picked for  $\omega = 0$  for a given  $\mu$  and  $T$ . This temperature then is the transition temperature  $T_c$  for a given  $\mu$ . The condition:

$$|\eta_l(\omega = 0, \mu, T)| = 1, \quad (16)$$

corresponds to the Thouless criterion for the critical temperature for a non-local interaction [37, 43]. While this technique has been used to get  $T_c$  for the uncoupled channel in [36], in this work, it has been extended for the coupled channel. In the next section, we present our results for both the  $^1S_0$  and the  $^3P_2 - ^3F_2$  channels.

### III. NUMERICAL RESULTS AT ZERO AND FINITE TEMPERATURES

We begin by studying the pairing gap at zero temperatures for the  $^1S_0$  and  $^3P_2 - ^3F_2$  channels using both the techniques of solving the BCS gap equation and the stability analysis. While the zero temperature  $^1S_0$  gaps within the BCS approximation are not new, it serves to benchmark the codes and the techniques.

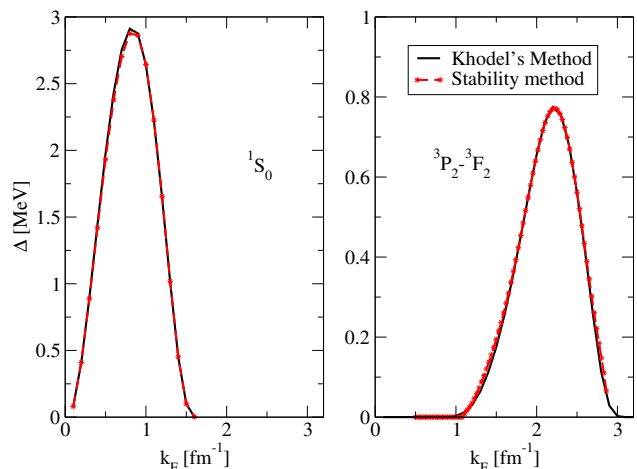


FIG. 1: (Color online) Zero temperature gap for the singlet (left) and the triplet (right) obtained from chiral N3LO potential [41]. The  $^1S_0$  gaps uses SRG evolved interaction at  $\lambda = 2.0 \text{ fm}^{-1}$ , while the  $^3P_2 - ^3F_2$  gaps has the unevaluated interaction as input. Obtaining the gaps for higher resolution scale for the  $^1S_0$  channel using the stability method is complicated due to the presence of short range components in the interaction, that is usually softened by the RG evolution [36].

Fig. 1 shows the zero temperature momentum independent gaps for the  $^1S_0$  and  $^3P_2 - ^3F_2$  channels for pure

neutron matter as a function of  $k_F$ . We have used the chiral N3LO potentials [41] as the input for the gap equation. The gap equation is first angle-averaged and then solved in a numerically stable way due to Khodel (see section II A) (solid lines in Fig. 1). We also show the zero temperature gaps obtained via the stability analysis (dashed-lines) and we note that the two methods agree. Our results for the triplet channel agree with those found in the literature for the chiral N3LO interactions [20].

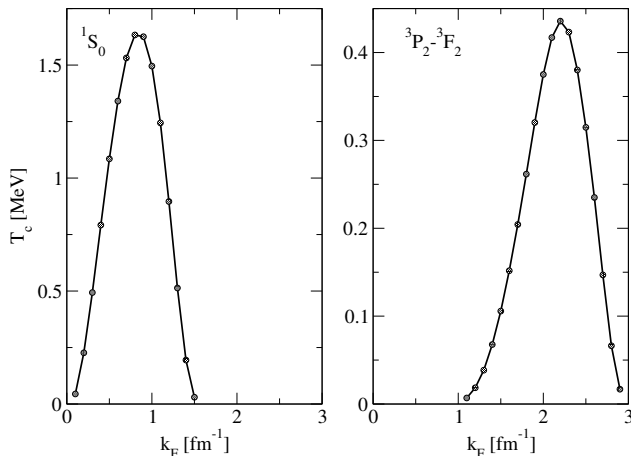


FIG. 2: Transition temperature as a function of  $k_F$  for the singlet (left) and the triplet (right) obtained from the chiral N3LO potential [41]. Again,  $T_c$  for the  $^1S_0$  channel uses the SRG evolved interaction with  $\lambda = 2.0 \text{ fm}^{-1}$ , while the triplet channel uses unevolved interaction as input.

Fig. 2 shows the transition temperature as a function of  $k_F$  for the chiral N3LO interaction obtained via the Thouless criterion in Eq. (16). The ratio of the zero temperature gap to the transition temperature follows the BCS result [33], i.e.

$$\frac{\Delta(k_F)}{T_c} \sim 1.76 \quad (17)$$

As outlined in the introduction, the strategy we adopt for the SRG resolution scale ( $\lambda$ ) dependence study of the triplet channel gaps is to use the SRG-evolved interactions as input for the gap equation. We wish to re-emphasize that the main motivation for using the SRG-evolved interactions for a given bare interaction is that the bare phase shifts are preserved and one can then attribute the  $\lambda$  dependence to the missing medium/many-body contributions. However, we will see the dependence on the bare interaction if we compare the results between different interactions, for example between N3LO and AV<sub>18</sub> and their corresponding SRG-evolved interactions. An alternative to this will be to compare the different models without the SRG evolution and include many-body/medium corrections until the results are model independent. But we wish to take advantage of the systematics that the EFT approach offers and hence we use the SRG-evolved interactions and study the resolution scale dependence for a given bare interaction.

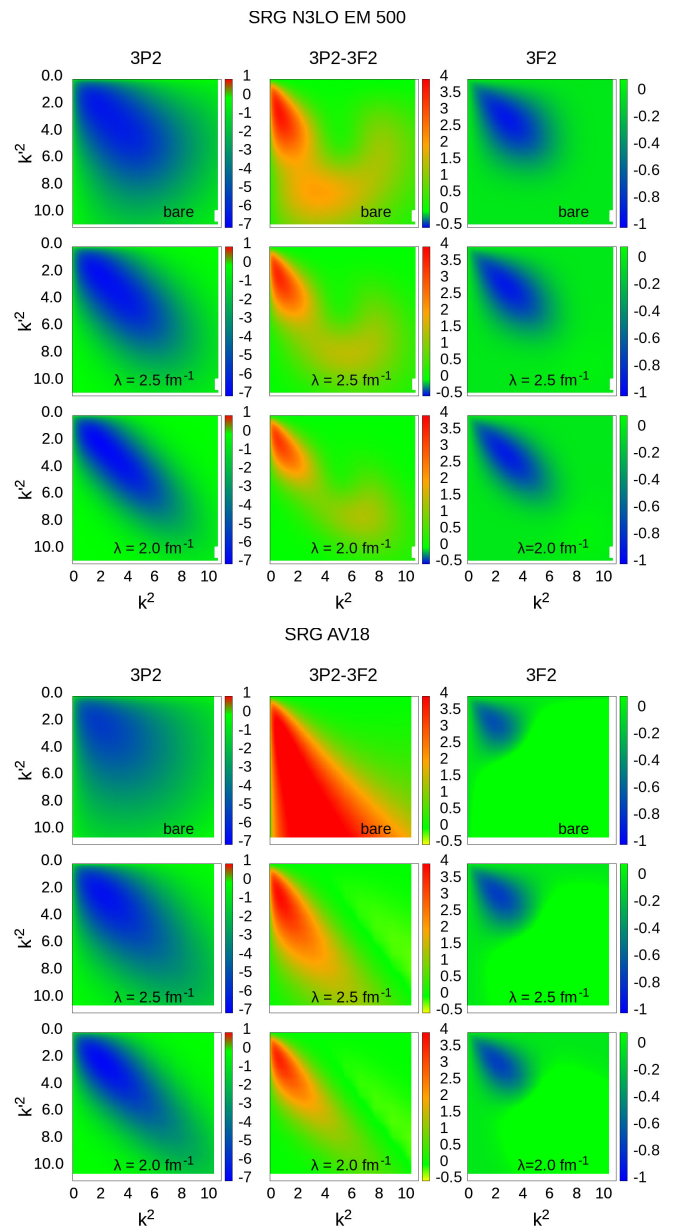


FIG. 3: (Color online) SRG-evolved  $^3P_2-^3F_2$  interactions as a function of  $k^2$  and  $k'^2$  for the N3LO EM 500 [41] interaction (top panel) and the AV<sub>18</sub> interaction (bottom panel). Note that the evolution drives the matrix elements towards the diagonal as function of the parameter  $\lambda$ .

We begin by revisiting the effect of the SRG evolution on the bare interaction. Fig. 3 shows the SRG evolution for the N3LO EM 500 [41] and the AV<sub>18</sub> [42] interactions in the triplet channel for pure neutron matter. We see that the evolution in both the cases, drives the interaction matrix elements towards the diagonal and this has consequences on the gaps, namely, the gaps decrease as the resolution scale  $\lambda$  decreases (see Fig. 5). In addition, the evolution preserves the bare phase shifts as it is uni-



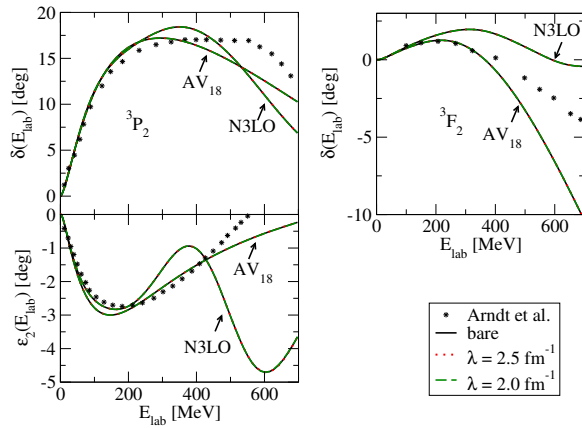


FIG. 4: (Color online) Comparing the phase shift in the triplet channel for the N3LO EM 500 [41] and the AV<sub>18</sub> [42] interaction. Note that the SRG evolution in each case preserves the phase shift as seen by the lack of dependence on the SRG resolution scale. For comparison, we have also included the partial wave analysis of the experimental phase shifts by Arndt et al. [29]

tary. This is seen in Fig. 4, where the phase shifts for different SRG resolution scales are identical to the bare (unevolved) phase shifts for both the N3LO EM 500 and the AV<sub>18</sub> interactions. In Fig. 4, we also show the partial wave analysis of the experimental  $NN$  scattering data of Arndt et al. [29] for comparison, and it is clearly seen that the phase shifts computed using the different  $NN$  interactions depart significantly from the experimental data at high energies. Hence when the triplet gaps from the different  $NN$  interactions are compared, the uncertainties in the calculated gaps also include the phase shift inequivalence that occur at higher energies in addition to the missing many-body/medium corrections. Therefore, we work with the AV<sub>18</sub> and the chiral N3LO interactions and their corresponding SRG evolved counterparts and we plan to study the  $\lambda$  dependence of the triplet gaps for a particular bare interaction. However, we note that the N3LO interaction cannot be trusted beyond the chiral EFT cut-off of  $2.5 \text{ fm}^{-1}$ , and conservatively, one should interpret the N3LO results beyond  $k_F \sim 2.0 \text{ fm}^{-1}$  with caution.

The triplet gaps at zero temperature for the SRG-evolved N3LO EM 500 and the evolved AV<sub>18</sub> interactions are seen in Fig. 5 in the top panel and bottom panel respectively, while Fig. 6 shows the  $\lambda$  dependence of the transition temperature obtained via the Thouless criterion (Eq. (16))<sup>1</sup>. We see that for both the N3LO and the AV18 class of interactions, lowering  $\lambda$  decreases the gap. This decrease can be linked to the changes the SRG evolution, determined by the generator, makes to the matrix elements, where the different  $ll'$  blocks are driven towards the diagonal (refer Fig. 3). Figs. 5 and 6 also document the SRG resolution scale dependence. We note that the results are independent of the SRG resolu-

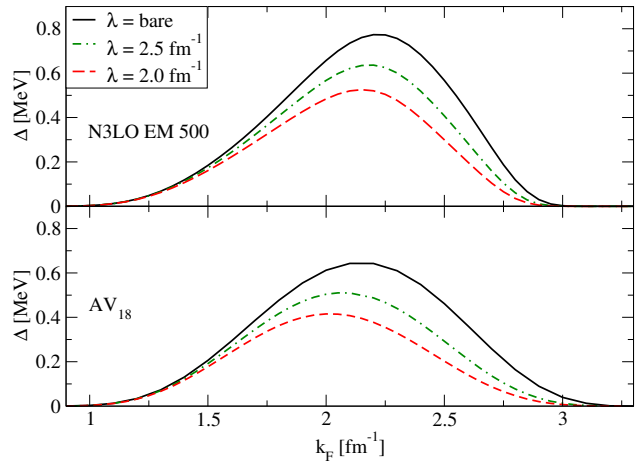


FIG. 5: (Color online) Zero temperature gaps obtained from N3LO EM 500 and AV<sub>18</sub> for different SRG resolution scales. The top panel has the N3LO EM 500 bare and SRG-evolved interactions as inputs. The bottom panel has the AV18 bare and SRG-evolved interactions for the same  $\lambda$  values.

tion scale for  $k_F \approx 1.3 \text{ fm}^{-1}$ . The same trends carry over to the transition temperature in Fig. 6. The  $\lambda$  dependence sets the scale of the missing many-body/medium corrections as a function of  $k_F$ .

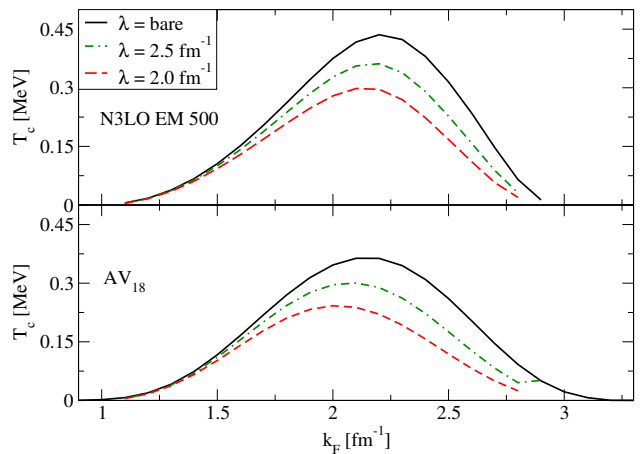


FIG. 6: (Color online) Transition temperature as a function of  $k_F$  for N3LO EM 500 and AV<sub>18</sub> for different SRG resolution scale. The top panel has the N3LO EM 500 bare and its SRG-evolved interactions as inputs. The bottom panel has the bare AV18 and its SRG-evolved interactions as inputs.

So far in our discussions, we use the free space inter-

[1] For the transition temperature using the bare AV<sub>18</sub> interaction, there were numerical issues beyond  $2.0 \text{ fm}^{-1}$  and the transition temperature as seen in Fig. 6 for the bare AV<sub>18</sub> alone is obtained from the BCS scaling. However, for the SRG-evolved AV<sub>18</sub> interaction as well as for the N3LO (bare and evolved), the Thouless criterion for the transition temperature turns out to be numerically stable.

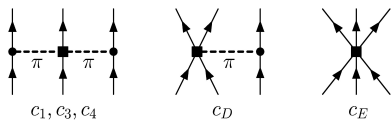


FIG. 7: Leading chiral 3N forces at N2LO [16].

action matrix elements (bare or equivalent SRG- evolved interactions) for the vertex. For the intermediate states the free particle spectrum is used. But at finite densities, corrections to both the vertex and the single-particle energy are important. Therefore, in this study we will include the 3N interaction as an effective density dependent 2N interaction as well as correct the free-particle spectrum with the first-order self-energy term. We begin by reviewing the 3N corrections to the vertex.

The three-body force has been in the past included via an effective two-body density dependent interaction [16, 18]. Following the previous work by Hebeler and Schwenk [16] for the  $^1S_0$  channel, we include the leading order chiral 3N interactions which occur at N2LO (Fig. 7). In pure neutron matter only the long-range two pion exchange diagram contributes and further in this diagram only the  $c_1$  and  $c_3$  terms contribute [16]. We use values of  $c_1 = -0.81 \text{ GeV}^{-1}$  and  $c_3 = -3.2 \text{ GeV}^{-1}$  [16, 41]. For the 3N interaction the following smooth regulator is used:

$$f_R(p, q) = \exp \left[ - \left( \frac{p^2 + 3q^2/4}{\Lambda_{3\text{NF}}^2} \right)^{n_{\text{exp}}} \right], \quad (18)$$

where  $p$  and  $q$  are the Jacobi momenta and  $\Lambda_{3\text{NF}}$  is the three-body cut-off and  $n_{\text{exp}}$  is the parameter for the exponential regulator. We use  $n_{\text{exp}} = 2$  in our study. Since we are including the long-range two pion force, we assume that it is not modified by the RG running and use the same values for  $c_1$  and  $c_3$  for different  $\Lambda_{3\text{N}}$  cut-off. In order to obtain the effective 2N interaction, we integrate the third particle over the states occupied in the Fermi sea (schematically shown in Fig. 8), which is then added to the two-body interaction with appropriate symmetry factors.

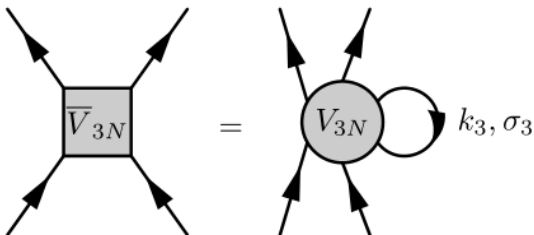


FIG. 8: Effective 2N generated by integrating the third particle over the states occupied in the Fermi sea.

For the BCS gap, the two body interaction augmented by the effective two-body term obtained from the 3N

force is given by [16]:

$$V_{\text{eff}}(k, k') = V_{2\text{N}}(k, k') + \frac{\bar{V}_{3\text{N}}(k, k')}{2}, \quad (19)$$

where  $\bar{V}_{3\text{N}}(k, k')$  denotes the effective density dependent 2N force. In addition to studying the dependence of the results on the SRG resolution scale, the three-body cut-off can be varied independently and the cut-off dependence of the results at the three-body level (which gives an estimate of the missing short-range three-body forces) can be analyzed.

Fig. 9 shows the zero temperature gap as a function of  $k_F$  when the input two-body interaction is augmented by the effective density dependent 2N force (solid lines). For comparison, the figure also shows the 2N only results (broken lines) as well. We note that for a given two-body resolution scale,  $\lambda$ , and three-body cut-off,  $\Lambda_{3\text{NF}}$ , the addition of the 3N force as a density dependent effective 2N interaction increases the triplet gaps (compare black solid and black broken lines). This increase in the gap is due to the attractive spin-orbit force that the effective 2N force adds to the input interaction [16]. Fig. 9 also shows the spread in the two-body resolution scale for a fixed three-body cut-off. It is observed that independent of the three-body cut-off, the two-body  $\lambda$  dependence is unaffected by the addition of the leading order three-body interaction. Therefore one is still missing important many-body corrections. In Fig. 9, we have restricted the density range to  $k_F < 2.0 \text{ fm}^{-1}$ . This limit for the density range is due to the fact that a leading order approximation for the 3N interaction has been used. Hence one cannot expect it to be valid at high densities. As mentioned in the introduction, the chiral interactions have a cut-off which in the case of N3LO EM 500 is around  $500 \text{ MeV} \sim 2.5 \text{ fm}^{-1}$  and the errors build up as this value is approached. Hence we use a conservative range for  $k_F$  values and restrict the range to  $< 2.0 \text{ fm}^{-1}$  when the 3N interactions are included. We would like to add in addition that we have neglected the induced 3N forces as we use unevolved 3N interactions and these are certainly important [24] and will be considered in a future publication.

To check the approximation made for the leading order effective three-body corrections, we compare in Fig. 10 the 3N cut-off dependence when the 2N resolution scale,  $\lambda$ , is held fixed. The results show strong dependence on  $\Lambda_{3\text{N}}$  thereby indicating that the short- and intermediate-range 3N effects are important for the range of densities considered. In fact, comparing Figs. 9 and 10, one sees that the results are more sensitive to the 3N cut-off compared to the 2N resolution scale. This in turn goes back to our motivation of restricting the densities in Figs. 9 and 10. Since the uncertainties with the 3N interaction is quite large within the approximation used here, we will not include the 3N corrections for the rest of the paper and will work with the NN-only vertex.

In order to correct for the single-particle spectrum we include the self-energy effects to first-order. Therefore,



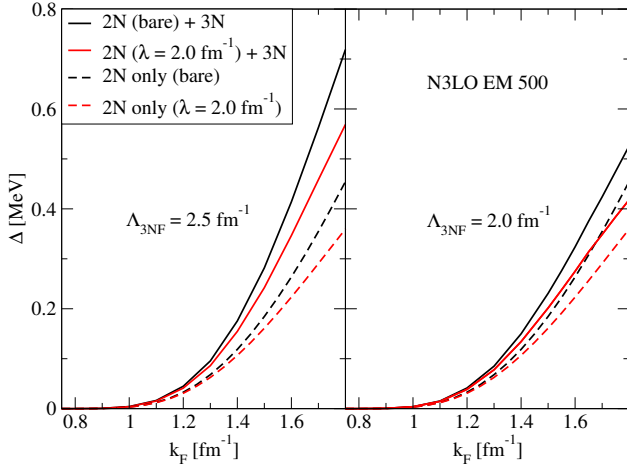


FIG. 9: (Color online) Two-body SRG resolution scale dependence for the N3LO EM 500, keeping  $\Lambda_{3NF}$  fixed when the two-body input is augmented by the effective 2N interaction.

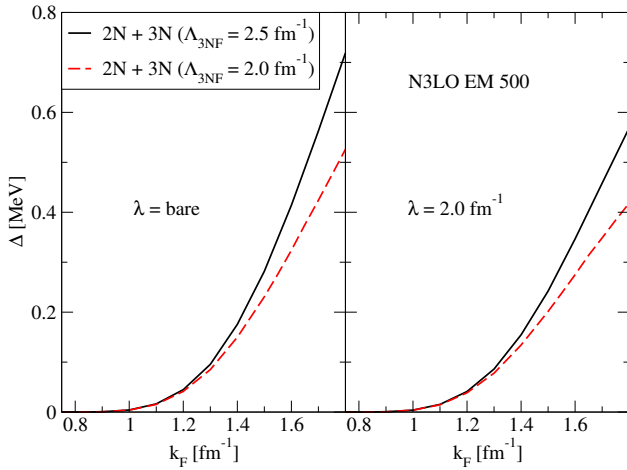


FIG. 10: (Color online) Three-body cut-off dependence for the N3LO EM 500, keeping the two-body SRG resolution scale  $\lambda$  fixed, when the two-body input is augmented by the effective 2N interaction.

the energy  $e(k)$  of the intermediate states become:

$$e(k) = \frac{k^2}{2} + \Sigma^{(1)}(k) \quad (20)$$

where  $\Sigma^{(1)}(k)$  is the static first-order contribution that is diagrammatically shown in Fig. 11.

The first-order term can be written in the partial wave basis as follows [16]:

$$\Sigma^{(1)}(k_1) = \frac{1}{2\pi} \int k_2^2 dk_2 \int d(\cos \theta_{\mathbf{k}_1, \mathbf{k}_2}) n_{\mathbf{k}_2} \sum_{l,S,J} (2J+1) \langle k_{12}/2 | V_{SUJ} | k_{12}/2 \rangle (1 - (-1)^{l+S+1}), \quad (21)$$

where  $n_{\mathbf{k}_2} = \theta(k_F - k_2)$  is the Fermi-Dirac distribution at zero temperature and  $k_{12} = |\mathbf{k}_1 - \mathbf{k}_2|$  and we align the

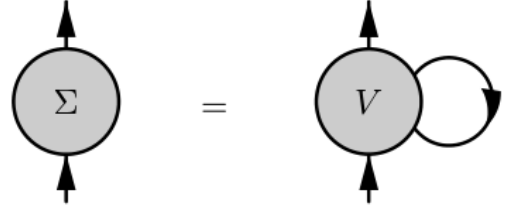


FIG. 11: First-order self-energy.

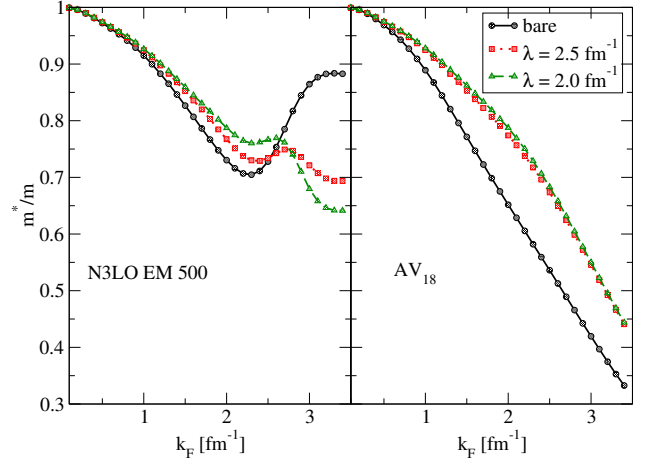


FIG. 12: (Color online) Effective mass using the first order self-energy term for N3LO EM 500 and AV<sub>18</sub> interactions for bare and different SRG resolution scales.

$z$  axis in the direction of  $\mathbf{k}_1$ . Since we are interested in the gaps at  $k_F$ , it is useful to study the effective mass  $m^*$  defined as (using units  $\hbar^2/m_N = 1$ )

$$\frac{m^*}{m} = \left( \frac{1}{k} \frac{de(k)}{dk} \right)^{-1} \Big|_{k=k_F}. \quad (22)$$

The effective mass is directly related to the density of states at  $k_F$  and a lower  $m^*/m$  indicates depletion of states at  $k_F$ .

Fig. 12 shows the  $k_F$  dependence of the effective mass, where the ratio  $m^*/m$  is plotted as a function of  $k_F$  for the N3LO EM 500 (left panel) and the AV<sub>18</sub> (right panel) as well as the respective SRG evolved interactions for  $\lambda = 2.5 \text{ fm}^{-1}$  and  $2.0 \text{ fm}^{-1}$ . The ratio of  $m^*/m$  as a function of density decreases for both the AV<sub>18</sub> and the N3LO EM 500 interactions as a function of  $k_F$ . However, for the N3LO interactions beyond  $2.0 \text{ fm}^{-1}$ , this ratio increases, although it is still less than 1. But beyond  $2.0 \text{ fm}^{-1}$ , the chiral interaction becomes unreliable as momenta/densities approach the chiral cut-off of  $2.5 \text{ fm}^{-1}$ . This is roughly where the systematics with the SRG evolution scale breaks down for the N3LO as seen in Fig. 12. For the AV<sub>18</sub> interaction, it is not surprising that the first order approximation to the self-energy is rather poor as

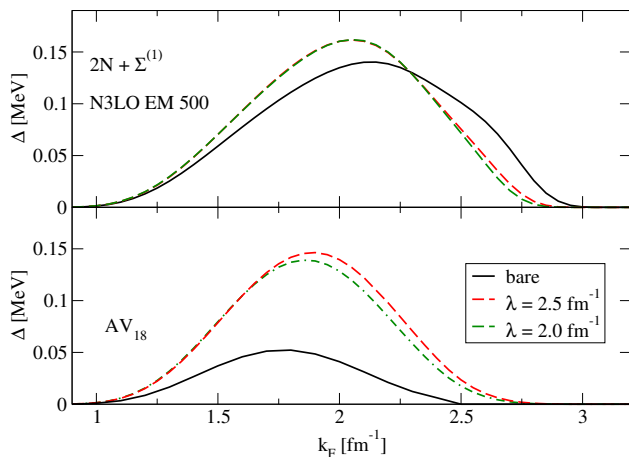


FIG. 13: (Color online) First-order self-energy effects on the zero temperature gap using N3LO EM 500 and AV18 respectively and the corresponding SRG-evolved interactions as inputs.

can be seen by the small values of  $m^*/m$  (compare with Fig. 5 of [14]). This is especially true with the bare which is known to be a hard interaction. For the SRG evolved AV<sub>18</sub> interactions the first order approximation for the self-energy is expected to break down at higher densities.

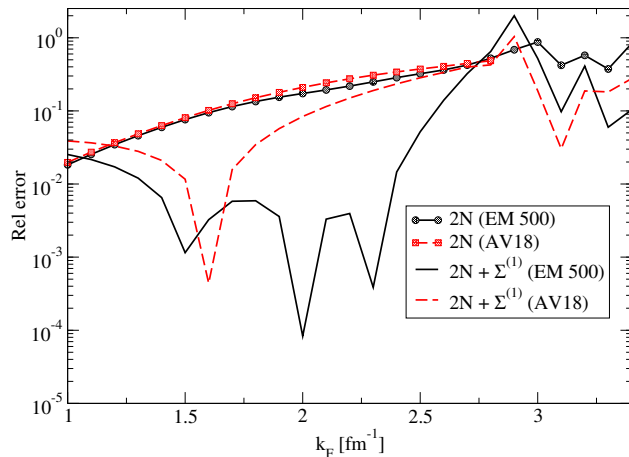


FIG. 14: (Color online) Relative error between the cut-offs ( $\Lambda = 2.0 \text{ fm}^{-1}$  and  $\Lambda = 2.5 \text{ fm}^{-1}$ ) for N3LO EM 500 and AV18 SRG-evolved interactions.

From the behavior of  $m^*/m$  as a function of  $k_F$ , one expects that with the first order self-energy correction as given in Eqs. (20) and (21), the triplet gaps should decrease in magnitude, which is what is observed in Fig. 13, compared to the ones with the free spectrum (see Fig. 5). Further, for the SRG evolved interactions, in each case, we note that the gaps increase in magnitude compared to the corresponding bare interaction (solid black line) in Fig. 13, which could be linked to the specifics of the SRG evolution. However, one needs to interpret the first-

order self-energy correction to the bare interaction with caution. In particular for the bare AV<sub>18</sub>, one sees that the gaps are very small compared to the SRG evolved counterparts. This drastic depletion of the gaps could indicate that the first order approximation for the self-energy for the bare AV<sub>18</sub> is rather poor. Similarly for the SRG evolved AV<sub>18</sub> interactions, one observes that the  $\lambda$  dependence sets in around  $k_F \sim 1.7 \text{ fm}^{-1}$ , thereby indicating the need for higher-order corrections for the self-energy. On the other hand, with the N3LO EM 500, while the differences between the bare interactions and the SRG evolved ones are not as striking as the AV<sub>18</sub>, one expects the first order correction to the self-energy to breakdown at higher  $k_F$ s, especially for the bare. The SRG evolved N3LO interactions are soft and one observes that the results have minimal cut-off dependence for  $k_F$  in the range  $[1.0 \text{ fm}^{-1} - 2.2 \text{ fm}^{-1}]$ , although one should interpret the N3LO results beyond  $k_F$  of  $2.0 \text{ fm}^{-1}$  with caution.

In order to better track the cut-off dependence, we study the relative errors in the zero temperature gaps as a function of  $k_F$  for the 2N-only results with (lines without symbols) and without (lines with symbols) the first order self-energy correction in Fig. 14 for the SRG evolved interactions. The relative error is obtained by taking the normalized differences of the zero temperature gaps at two different SRG resolution scales for the N3LO and AV<sub>18</sub> interactions. Not taking into account the densities where the gap opens (or any accidental cancellations in the relative error), we note that there is an overall reduction in the relative error for densities less than  $2.0 \text{ fm}^{-1}$  when a first order self-energy correction is used (lines without symbols) compared to the case where a free spectrum is used for the intermediate states. At higher densities, higher order corrections to the self-energy become important. The reduction in the relative errors for the AV<sub>18</sub> interaction is not on the same scale when compared with the chiral interaction and this could be due to the differences between the phenomenological and EFT based interactions. Therefore, from Figs. 13 and 14, one can conclude that the addition of self-energy effects, although at first order, decreases the resolution scale dependence and is an important correction.

Another striking feature of including the self-energy correction is that the gap closure shifts to lower densities as seen in Figs. 13 and 15. The shift is similar to the one observed when short range correlations (SRCs) are included in the interaction (Fig. 10 [21]). The effects of self-energy versus the free-spectrum is examined in detail in Fig. 15, where we use a log-scale to better document the effects of the cut-off as well to understand the impact of the first order self-energy correction on the gap closure. Ding et al. [20, 21] observe a lowering of the gap and a shift in the gap closure to lower densities when they include short-range correlations within a self-consistent Greens function theory. For the N3LO EM 500 one cannot conclude much about the closure, but for the AV<sub>18</sub> interaction, we note that the gap closes at

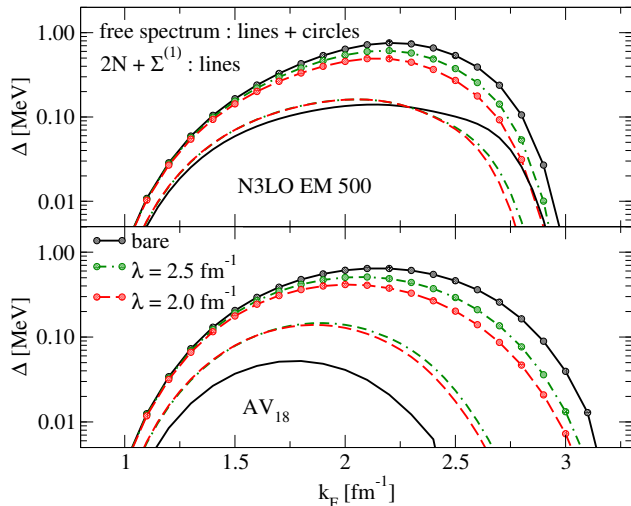


FIG. 15: (Color online) Effect of first-order self-energy versus the free spectrum for N3LO (top panel) and AV<sub>18</sub> (bottom panel). The log-scale details the effects of SRG running on the gaps as well as the closure.

lower  $k_F$  when the self-energy at first-order is included, although the closure is at a higher density compared to the Ding et al results. We note and emphasize that a first order correction to the self-energy may not be sufficient to comment without ambiguities about gap closures. It would be interesting to study the effects of second order self-energy as well as higher order effects systematically on the gaps in the triplet channel.

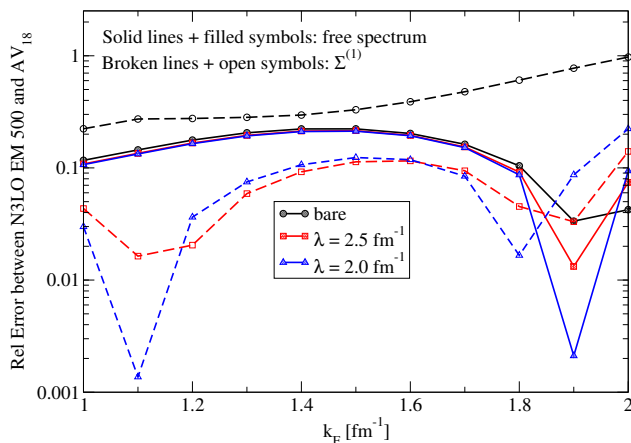


FIG. 16: (Color online) Relative error between N3LO EM 500 and AV<sub>18</sub> interactions for different cut-offs including the bare interaction with and without the self-energy corrections. The solid lines with filled symbols are the relative errors for the free spectrum, while the broken lines with the open symbols include self-energy corrections to first-order.

We have been emphasizing that the triplet gaps ob-

tained thus far will depend on the interaction used in the BCS gap equation as the densities are very high and the interactions are not phase-shift equivalent in free space. In addition, one cannot expect the free-space interaction to completely describe the pairing in the triplet channel. As an attempt to track the dependence of the results on the free-space interaction, we study the relative error, which are normalized differences between gaps obtained from the N3LO EM 500 and AV<sub>18</sub> interactions for the bare and the two different SRG resolution scales in Fig. 16 with and without the self-energy corrections. We only document the results for  $k_F < 2.0 \text{ fm}^{-1}$ , that is within the conservative estimate for the validity of the free space N3LO interactions. With a free spectrum (solid lines with filled symbols), there is not much difference in the relative error between the bare and the SRG evolved interactions except for  $k_F$  close to  $2.0 \text{ fm}^{-1}$ . When the first order self energy correction is included, the error between the N3LO and AV<sub>18</sub> is quite large when the bare interactions are compared, but that decreases once the interactions are SRG evolved to lower  $\lambda$  values. All the same, compared to Fig. 14, the relative errors between the models are quite large and this can be attributed to the fact that the interactions are not phase shift equivalent (see Fig. 4). In fact, by comparing the N3LO interaction with a phenomenological one, we see the effects of free space phase shift inequivalence on the triplet gaps, which ties well with our motivation to study the gaps as a function of the SRG resolution scale instead.

#### IV. CONCLUSIONS

The goal of this work is to understand the pairing physics of the triplet channel in pure neutron matter. We use SRG-evolved interactions as inputs as they preserve the bare phase shifts by construction and hence the phase shift inequivalence is factored out of the results and one can attribute the resulting dependence on the SRG resolution scale  $\lambda$  to the missing many-body/medium effects.

The zero temperature gaps are obtained by solving the angle-averaged BCS gap equation using the numerically stable procedure of Khodel et al as well as by the stability method that locates the pole of the in-medium  $T$  matrix. We also obtain the transition temperature using the Thouless criterion generalized for non-local interaction and verify that  $\frac{\Delta(k_F)}{T_c} \sim 1.76$  at the BCS level.

The gaps should be independent of the SRG resolution scale  $\lambda$  and therefore, any  $\lambda$  dependence is used as a tool to estimate the missing many-body/medium corrections. To this effect, we included the three-body effects at leading order via a density dependent effective two-body interaction. Including the three-body term at leading order does not change the two-body  $\lambda$  dependence and further, we note via the dependence on the  $3N$  cut-off that the

short-range three-body effects are important. As a result, given these uncertainties with the leading order  $3N$ , we have not included the  $3N$  corrections to the self-energy studies.

The self-energy at first-order is included and this results in significant changes in the overall values of the gaps, gap closure as well as reduced  $\lambda$  dependence. In fact, with the first order self-energy correction we see trends similar to that observed in the literature when short-range correlations are included [17, 20, 21]. However, we would like to emphasize that higher-order corrections to the self-energy are important.

These results are encouraging at this point and it would be interesting to further investigate systematically, higher-order many-body/medium effects using the EFT approach and this is currently in progress.

### Acknowledgments

We would like to thank Dick Furnstahl, Michael Urban, Kai Hebeler and Christian Drischler for useful comments and suggestions. We would like to acknowledge the contribution of Kai Hebeler who provided the three-body matrix elements and Christian Drischler who provided us the data for benchmarking our codes. We would like to thank Paolo Finelli, Stefano Maurizio and Wilhem Dickhoff who discussed with us their results and numerical implementation in detail. SR acknowledges support from the New Faculty Seed Grant from IIT Madras which provided the infrastructure to carry out the numerical calculations in this paper.

### Appendix: SRG Evolution

Similarity Renormalization Group [39, 40] achieves the decoupling of low- and high-momentum modes using unitary transformations of the Hamiltonian. This has the unique feature of driving the high-momentum states towards the diagonal, which makes it different from the RG methods so far seen. The low-momentum effective potential obtained using Similarity Renormalization Group (SRG) denoted as  $V_{\text{SRG}}$ , preserves all the phase shifts with respect to the bare potential.

Consider the following transformation on the hamiltonian

$$H_s = U(s)HU^\dagger(s) \equiv T_{\text{rel}} + V_s \quad (\text{A.1})$$

where  $U(s)$  and  $U^\dagger(s)$  are unitary operators. Now

$$\frac{dH_s}{ds} = \frac{dU_s}{ds}HU^\dagger(s) + U(s)H\frac{dU^\dagger}{ds}. \quad (\text{A.2})$$

Defining  $\eta(s) = \frac{dU(s)}{ds}U^\dagger(s)$ , Eq. (A.2) becomes,

$$\frac{dH_s}{ds} = \eta(s)H_s + H_s\eta^\dagger(s). \quad (\text{A.3})$$

Using  $U^\dagger(s)U(s) = 1$ , one can establish that  $\eta^\dagger(s) + \eta(s) = 0$ , so that, Eq. (A.3) can be written as,

$$\frac{dH_s}{ds} = \eta(s)H_s - H_s\eta(s) = [\eta(s), H_s]. \quad (\text{A.4})$$

We have the freedom to choose  $\eta(s)$  and the canonical choice is [40]:

$$\eta(s) = [T_{\text{rel}}, H_s] = \frac{dU(s)}{ds}U^\dagger(s). \quad (\text{A.5})$$

The flow equation given by Eq (A.4) now reads:

$$\frac{dH_s}{ds} = [[T_{\text{rel}}, H_s], H_s]. \quad (\text{A.6})$$

After some algebra one can show that Eq. (A.6) reduces to

$$\begin{aligned} \frac{dV_s(k', k)}{ds} &= -(k^2 - (k')^2)^2 V_s(k', k) \\ &+ \frac{2}{\pi} \int_0^\lambda q^2 dq (k^2 + (k')^2 - 2q^2) V_s(k', q) V_s(q, k) \end{aligned} \quad (\text{A.7})$$

Far away from the diagonal, the first term in Eq. (A.7) dominates, that is:

$$\frac{dV_s(k', k)}{ds} \approx -(k^2 - (k')^2)^2 V_s(k', k), \quad (\text{A.8})$$

so that,

$$V_s(k', k) \approx V_0(k', k)e^{-(k^2 - k'^2)^2 s}. \quad (\text{A.9})$$

Therefore it is clear that the off-diagonal elements are exponentially suppressed. Using the fact that  $s^{-1/4}$  has the dimensions of momentum, one can define  $\lambda = s^{-1/4}$ , where  $\lambda$  measures the spread of the off-diagonal strength.

[1] N. Chamel and P. Haensel, Living Rev. Relativity **11**, 10 (2008) [<http://www.livingreviews.org/lrr-2008-10>].  
 [2] O. Y. Gnedin, D. G. Yakovlev and A. Y. Potekhin, Mon. Not. Roy. Astron. Soc. **324**, 725 (2001) doi:10.1046/j.1365-8711.2001.04359.x [astro-ph/0012306].

[3] D. G. Yakovlev and C. J. Pethick, Ann. Rev. Astron. Astrophys. **42**, 169 (2004).  
 [4] C. Monrozeau, J. Margueron and N. Sandulescu, Phys. Rev. C **75**, 065807 (2007).  
 [5] D. G. Yakovlev, O. Y. Gnedin, A. D. Kaminker and A. Y. Potekhin, AIP Conf. Proc. **983**, 379 (2008)

- doi:10.1063/1.2900259 [arXiv:0710.2047 [astro-ph]].
- [6] D. D. Ofengeim, A. D. Kaminker, D. Klochkov, V. Suleimanov and D. G. Yakovlev, *Mon. Not. Roy. Astron. Soc.* **454**, no. 3, 2668 (2015) doi:10.1093/mnras/stv2204, arXiv:1510.00573 [astro-ph.SR].
- [7] D. Page, J. M. Lattimer, M. Prakash and A. W. Steiner, *Astrophys. J. Suppl.* **155**, 623 (2004) doi:10.1086/424844, [astro-ph/0403657].
- [8] D. Page, J. M. Lattimer, M. Prakash and A. W. Steiner, *Astrophys. J.* **707**, 1131 (2009) doi:10.1088/0004-637X/707/2/1131 [arXiv:0906.1621 [astro-ph.SR]].
- [9] D. Page, M. Prakash, J. M. Lattimer and A. W. Steiner, *Phys. Rev. Lett.* **106**, 081101 (2011) doi:10.1103/PhysRevLett.106.081101 [arXiv:1011.6142 [astro-ph.HE]].
- [10] W. C. G. Ho and C. O. Heinke, *Nature* **462**, 71 (2009) doi:10.1038/nature08525 [arXiv:0911.0672 [astro-ph.HE]].
- [11] C. O. Heinke and W. C. G. Ho, *Astrophys. J.* **719**, L167 (2010) doi:10.1088/2041-8205/719/2/L167 [arXiv:1007.4719 [astro-ph.HE]].
- [12] K. G. Elshamouty, C. O. Heinke, G. R. Sivakoff, W. C. G. Ho, P. S. Shternin, D. G. Yakovlev, D. J. Patnaude and L. David, *Astrophys. J.* **777**, 22 (2013) doi:10.1088/0004-637X/777/1/22, [arXiv:1306.3387 [astro-ph.HE]].
- [13] K. Hebeler, A. Schwenk, and B. Friman, *Phys. Lett. B* **648**, 176 (2007).
- [14] M. Baldo, O. Elgaroey, L. Engvik, M. Hjorth-Jensen and H. J. Schulze, *Phys. Rev. C* **58**, 1921 (1998) doi:10.1103/PhysRevC.58.1921 [nucl-th/9806097].
- [15] D. J. Dean and M. Hjorth-Jensen, *Rev. Mod. Phys.* **75**, 607 (2003) doi:10.1103/RevModPhys.75.607 [nucl-th/0210033].
- [16] K. Hebeler and A. Schwenk, *Phys. Rev. C* **82**, 014314 (2010).
- [17] J. M. Dong, U. Lombardo and W. Zuo, *Phys. Rev. C* **87**, no. 6, 062801 (2013) doi:10.1103/PhysRevC.87.062801 [arXiv:1304.0117 [nucl-th]].
- [18] S. Maurizio, J. W. Holt and P. Finelli, *Phys. Rev. C* **90**, no. 4, 044003 (2014) [arXiv:1408.6281 [nucl-th]].
- [19] P. Finelli, S. Maurizio and J. W. Holt, *EPJ Web Conf.* **95**, 04021 (2015) doi:10.1051/epjconf/20159504021 [arXiv:1411.7504 [nucl-th]].
- [20] D. Ding, A. Rios, W. H. Dickhoff, H. Dussan, A. Polls and S. J. Witte, arXiv:1502.05673 [nucl-th].
- [21] D. Ding, A. Rios, H. Dussan, W. H. Dickhoff, S. J. Witte and A. Polls, arXiv:1601.01600 [nucl-th].
- [22] X. R. Zhou, H.-J. Schulze, E. G. Zhao, F. Pan and J. P. Draayer, *Phys. Rev. C* **70**, 048802 (2004). doi:10.1103/PhysRevC.70.048802
- [23] W. Zuo, C. X. Cui, U. Lombardo and H.-J. Schulze, *Phys. Rev. C* **78**, 015805 (2008). doi:10.1103/PhysRevC.78.015805
- [24] K. Hebeler and R. J. Furnstahl, *Phys. Rev. C* **87**, no. 3, 031302 (2013) doi:10.1103/PhysRevC.87.031302 [arXiv:1301.7467 [nucl-th]].
- [25] M. Hoffberg, A. E. Glassgold, R. W. Richardson, and M. Ruderman *Phys. Rev. Lett.* **24**, 775 (1970).
- [26] Ryozo Tamagaki, *Prog. Theor. Phys.* **44**, 905 (1970). doi:10.1143/PTP.44.905
- [27] R. W. Richardson, *Phys. Rev. D* **5**, 1883 (1972).
- [28] P. F. Bedaque and A. N. Nicholson, *Phys. Rev. C* **87**, no. 5, 055807 (2013) Erratum: [*Phys. Rev. C* **89**, no. 2, 029902 (2014)] doi:10.1103/PhysRevC.89.029902, 10.1103/PhysRevC.87.055807 [arXiv:1212.1122 [nucl-th]].
- [29] R. A. Arndt, C. H. Oh, I. I. Strakovsky, R. L. Workman and F. Dohrmann, *Phys. Rev. C* **56**, 3005 (1997) doi:10.1103/PhysRevC.56.3005 [nucl-th/9706003].
- [30] V. V. Khodel, V. A. Khodel and J. W. Clark, *Nucl. Phys. A* **679**, 827 (2001) [nucl-th/0001006].
- [31] S. Weinberg, *Phys. Rev.* **131** 440 (1963).
- [32] S. K. Bogner, R. J. Furnstahl, S. Ramanan, and A. Schwenk, *Nucl. Phys.* **A773** (2006) 203.
- [33] “Quantum Theory of Many-particle systems”, Alexander L. Fetter and John Dirk Walecka, Dover Publications, ISBN:978-0486428277 –
- [34] “Methods of Quantum Field theory in Statistical Physics”, A. A. Abrikosov, L. P. Gorkov and I. E. Dzyaloshinski, Dover Publication Inc., ISBN:978-0486632285
- [35] “Many-Body Theory Exposed!”, Willem H. Dickhoff and Dimitri Van Neck, World Scientific Publishing Company, ISBN: 978-9812813800
- [36] S. Ramanan, S. K. Bogner, and R. J. Furnstahl, *Nucl. Phys. A* **797**, 81 (2007).
- [37] S. Ramanan and M. Urban, *Phys. Rev. C* **88**, no. 5, 054315 (2013) [arXiv:1308.0939 [nucl-th]].
- [38] R. J. Furnstahl and K. Hebeler, *Rept. Prog. Phys.* **76**, 126301 (2013) doi:10.1088/0034-4885/76/12/126301 [arXiv:1305.3800 [nucl-th]].
- [39] S. K. Bogner, R. J. Furnstahl and A. Schwenk, *Prog. Part. Nucl. Phys.* **65**, 94 (2010) doi:10.1016/j.pnpnp.2010.03.001 [arXiv:0912.3688 [nucl-th]].
- [40] S. K. Bogner, R. J. Furnstahl and R. J. Perry, *Phys. Rev. C* **75**, 061001 (2007) doi:10.1103/PhysRevC.75.061001 [nucl-th/0611045].
- [41] D. R. Entem and R. Machleidt, *Phys. Rev. C* **68**, 041001 (2003) [nucl-th/0304018].
- [42] R. B. Wiringa, V. G. J. Stoks, and R. Schiavilla *Phys. Rev. C* **51**, 3851 (1995)
- [43] D. J. Thouless, *Ann. Phys. (N.Y.)* **10**, 553 (1960).
- [44] E. Krotscheck, *Z. Physik*, **251**, 135 (1972)